

Short communication

## Enhancement of aldehyde-water shift reaction over CuZnAl catalyst by Mn promoter

Tongqi Ye<sup>a,\*</sup>, Yue Ai<sup>a</sup>, Bao Chen<sup>a</sup>, Yuewen Ye<sup>a</sup>, Jia Sun<sup>b</sup>, Ling Qin<sup>a</sup>, Xin Yao<sup>a</sup><sup>a</sup> Anhui Province Key Laboratory of Advanced Catalytic Materials and Reaction Engineering, School of Chemistry and Chemical Engineering, Hefei University of Technology, Hefei, Anhui, 230009, PR China<sup>b</sup> Cardiff Catalysis Institution, Cardiff University, Cardiff, CF24 0HW, UK

## ARTICLE INFO

## Keywords:

MnCuZnAl catalyst  
Aldehyde-water shift  
Propanal  
Propanoic acid

## ABSTRACT

A series of Mn promoted CuZnAl catalysts were prepared by coprecipitation method. Doping of manganese in CuZnAl strongly enhanced the AWS activity and propionic acid selectivity. The interaction between Cu and Mn ions results in suppressed the hydrogenation of propanal to propyl alcohol and enhanced the selectivity of propionic acid. According to our results, the most favorable Mn/Cu molar ratio is 1:1. Higher temperature is also beneficial to the selectivity of propionic acid on CuZnAl-based catalysts.

## 1. Introduction

Bio-based alcohols and aldehydes such as ethanol, furfural, glycerol can be further oxidized to corresponding carboxylic acids with O<sub>2</sub>. Nowadays, in order to economize and optimize the process of biomass conversion and utilization, a growing interest has been focused on finding new reaction process. In this background, soft oxidation routes using weak oxidants such as H<sub>2</sub>O, CO<sub>2</sub> and N<sub>2</sub>O are attracting more and more attentions [1–5]. With those weak oxidants, reactions can be more gently and catalytic combustion can be depressed to enhance the selectivity of desired products. Aldehyde-water shift (AWS) reaction, is one of the typical oxidation process works with weak oxidants. In an AWS reaction, the aldehyde react with water to produce corresponding carboxylic acid and hydrogen (RCHO + H<sub>2</sub>O ↔ RCOOH + H<sub>2</sub>). Water works as a reaction partner, one proton is to form molecular hydrogen while the hydroxyl group is incorporated into the carboxylic acid [6]. Complete oxidation to CO<sub>2</sub> or CO can be safely suppressed (except for the steam reforming at high temperatures).

Several works focusing on AWS reaction have been published in the past few years. Brewster etc. reported a series of half-sandwich complexes of Ir, Rh, and Ru are shown to be active catalysts for the AWS of alkyl and aromatic aldehydes [2,3]. However, the homogeneous catalytic process and the usage of noble metals minimize the possibility toward industrialization. Orozco etc. proposed the AWS reaction as a step of heptanal ketonization on the CeO<sub>2</sub>-based heterogeneous catalysts [7]. Wen etc. suggested that reducible support may be beneficial to AWS

reaction [8]. They explored the AWS reaction of acetaldehyde on some oxide-supported metal catalysts, in which the Cu/CeO<sub>2</sub> and CuZnAl performed best. They pointed out that the synergistic effect of Cu sites and sites from reducible oxide of CeO<sub>2</sub> and ZnO is the key for the enhanced performance. However, the role of promoters and the way to improve the product selectivity are still matters worth investigation.

CuMn-based catalysts have attracting more and more attention recently. Manganese could adjust the electronic properties of copper through inner redox equilibrium (Cu<sup>2+</sup> + Mn<sup>3+</sup> ↔ Cu<sup>+</sup> + Mn<sup>4+</sup>). This property may be beneficial to the redox catalytic reactions [9]. The Cu–Mn mixed oxides have been applied in many catalytic reactions, such as catalytic removal of nitrogen oxides [10], water-gas shift reaction [11], steam reforming of methanol [12,13], total oxidation of propane and ethanol [14]. In this study, manganese oxides were introduced into the CuZnAl-based catalyst to enhance the AWS reaction and make further understanding of structure-function relationships of Cu active sites.

## 2. Experimental

## 2.1. Catalyst preparation

The mixed oxide catalysts were prepared by co-precipitation method using respective metal nitrate (AR, Sinopharm) solutions as precursors (1 mol/l of metal ions). The mixture solution of NaOH (AR) and Na<sub>2</sub>CO<sub>3</sub> (AR) (both 0.5 mol/L) was used as precipitator. The two solutions were

\* Corresponding author.

E-mail address: [yetq@hfut.edu.cn](mailto:yetq@hfut.edu.cn) (T. Ye).<https://doi.org/10.1016/j.catcom.2020.106262>

Received 5 October 2020; Received in revised form 25 November 2020; Accepted 27 November 2020

Available online 30 November 2020

1566-7367/© 2020 The Authors.

Published by Elsevier B.V. This is an open access article under the CC BY-NC-ND license

<http://creativecommons.org/licenses/by-nc-nd/4.0/>.

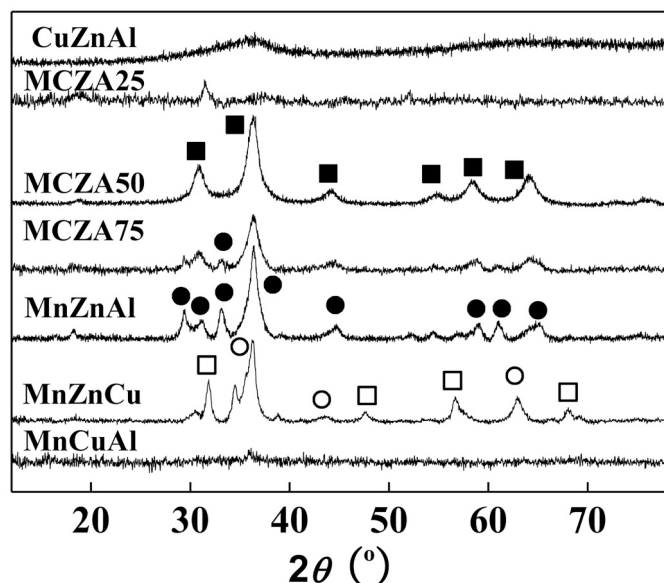


Fig. 1. XRD patterns of fresh catalysts (■spinel-like  $\text{Cu}_x\text{Zn}_{1-x}\text{Mn}_2\text{O}_4$ ; ● $\text{ZnMn}_2\text{O}_4$ ; ○ $\text{CuMn}_2\text{O}_4$ ; □ $\text{ZnO}$ ).

added dropwise to the stirred deionized water at  $50\text{ }^\circ\text{C}$  and  $\text{pH} = 9 \pm 0.2$ . The precipitate was aged in the mother liquor for 4 h. Thereafter filtered, washed with deionized water to  $\text{pH} 7$  and dried at  $110\text{ }^\circ\text{C}$  overnight. The precursors were then calcined at  $450\text{ }^\circ\text{C}$  for 3 h in muffle furnace with temperature ramp of  $1\text{ }^\circ\text{C}/\text{min}$  to obtain the corresponding mixed oxide catalysts. The latter ones were finally made into granules with 80–100 mesh sizes. The molar ratio of all ternary samples is 1:1:1 and named with their constituent elements. As for the quaternary samples, the molar ratio of (Mn + Cu): Zn: Al is 1:1:1. They were denoted as MCZAn (n is the molar ratio of Mn/(Mn + Cu)  $\times$  100%).

## 2.2. Catalyst characterization

An ICP-AES (Optima 7300 DV, Perkin Elmer, Korea) was used for the determination of compositions of fresh prepared catalysts. The surface area, pore size distribution and pore volume were determined by nitrogen adsorption at temperature of  $-196\text{ }^\circ\text{C}$ , using an Autosorb-IQ3 instrument. Powder X-ray diffraction (XRD) patterns were recorded on a PANalytical X-pert Pro MPD with a  $\text{Cu K}\alpha$  radiation ( $\lambda = 0.154\text{ nm}$ ). The surface elements and their states were analyzed by X-ray photoelectron spectroscopy (XPS) implemented on an ESCALAB-250Xi (Thermo-VG Scientific, USA) spectrometer with  $\text{Al K}\alpha$  ( $1486.6\text{ eV}$ ) irradiation source, using the C 1 s line at  $284.6\text{ eV}$  as the standard.

Temperature programmed reduction (TPR) and copper dispersion for

mixed oxide catalysts were carried out on a home-made apparatus that we used in previous work [6]. The calculation methods are also same with before except for the copper dispersion. The copper dispersion here is calculated by surface Cu divided by total Cu amount in the catalyst. The surface Cu is determined by TPR after pre-reduction and  $\text{N}_2\text{O}$  chemisorptions (see the supporting information for details). The total Cu amount is decided by ICP-AES instead of by TPR in normal method, because manganese could be partly reduced together with Cu as run the TPR.

## 2.3. Catalytic test

The AWS reaction of propanal was carried out in a quartz fixed-bed reactor at 260 and  $300\text{ }^\circ\text{C}$  respectively under atmospheric pressure. In a typical experiment, 0.1 g of the catalyst was introduced into the reactor. The catalyst bed was packed with silica wool which serves as the pre-heated zone. Prior to the reaction, the catalysts were pre-reduced by  $\text{H}_2$  stream at  $300\text{ }^\circ\text{C}$  for 2 h. Propanal ( $0.137\text{ g/h}$ ) and water ( $1.37\text{ g/h}$ ) were fed separately into the reactor using two syringe pumps during the reaction. High purity nitrogen (99.999%) was used as carrier gas in the experiments, keeping constant flow rate ( $10\text{ ml/min}$ ) by using mass flow controllers. The liquid product was condensed with an ice bath and analyzed offline by GC with an Agilent 7820 apparatus equipped with a PEG-20 M capillary column and a flame ionization detector (FID). The gaseous products were trapped in a gas burette and analyzed by GC equipped with a TCD detector connected to a Porapak Q packed column.

## 3. Results and discussion

### 3.1. Characterization of as prepared catalysts

XRD analysis was carried out to identify the phase of fresh prepared mixed oxide catalysts. As can be seen from Fig. 1, the XRD patterns are strongly affected by the catalyst compositions. No obvious diffraction peak was found in CuZnAl. The peaks at  $30.8$ ,  $36.4$ ,  $44.4$ ,  $54.9$ ,  $58.5$  and  $64.2$  which could be attributed to a spinel-like phase were observed in MCZA50 [15,16]. However, with the increasing of Mn/Cu molar ratio, the diffraction intensity decreased, together with the  $\text{ZnMn}_2\text{O}_4$  characterization diffraction peaks emerged, until the pure  $\text{ZnMn}_2\text{O}_4$  (JCPDS 77-0740) phase in MnZnAl sample. This indicates Cu and Mn are responsible for the formation of the spinel-like phase. Additionally, when we compared the MnZnCu and MnCuAl samples, we found that Zn is also essential for spinel-like structure. According to the reported works on CuMnZn mixed oxides [17,18], a spinel-like phase solid solution with formula of  $\text{Cu}_x\text{Zn}_{1-x}\text{Mn}_2\text{O}_4$  may formed in such a complex system and the XRD patterns are strongly influenced by Cu/Mn molar ratio. In the present work, the favorable molar ratio of Cu/Mn for the formation of spinel-like solid solution is around 1 in these quaternary samples. There's no signal of simple oxide of  $\text{CuO}$ ,  $\text{MnO}_2$ ,  $\text{ZnO}$  or  $\text{Al}_2\text{O}_3$

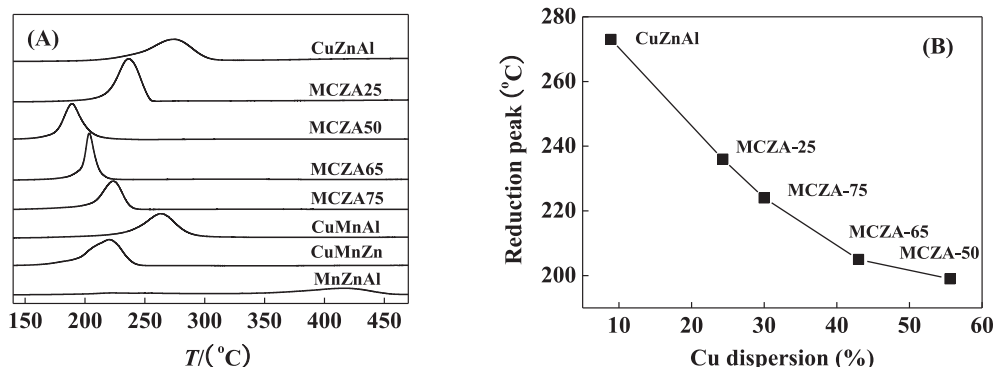


Fig. 2. TPR profiles of fresh MnCuZnAl catalysts (A), and the relationship between reduction peak ( $T_{\text{max}}$ ) and surface Cu dispersion (B).

**Table 1**  
Nitrogen adsorption-desorption and XPS analysis of MnCuZnAl catalysts.

Catalysts	Composition (mol%)	$S_{BET}$ ( $m^2 \cdot g^{-1}$ )	$PS^a$ (nm)	$PV^b$ ( $cm^3 \cdot g^{-1}$ )	Surface metals (%)				BE of fresh catalysts (eV)			
					Cu	Mn	Zn	Al	Cu (2p <sub>3/2</sub> )	Mn (2p <sub>3/2</sub> )	Zn (2p <sub>3/2</sub> )	Al (2p <sub>3/2</sub> )
CuZnAl	Cu <sub>36</sub> Zn <sub>34</sub> Al <sub>30</sub>	42.9	14.0	0.223	27	–	36	37	934.1	–	1021.9	73.9
MCZA25	Mn <sub>11</sub> Cu <sub>26</sub> Zn <sub>34</sub> Al <sub>29</sub>	91.3	9.33	0.255	23	10	38	29	934.2	642.1	1021.8	73.8
MCZA50	Mn <sub>19</sub> Cu <sub>17</sub> Zn <sub>34</sub> Al <sub>30</sub>	110.5	28.4	0.266	16	14	39	31	934.1	642.3	1021.4	73.5
MCZA65	Mn <sub>25</sub> Cu <sub>12</sub> Zn <sub>33</sub> Al <sub>30</sub>	108.3	25.1	0.247	11	16	38	35	934.1	642.4	1021.6	73.6
MCZA75	Mn <sub>28</sub> Cu <sub>10</sub> Zn <sub>33</sub> Al <sub>29</sub>	110.9	27.2	0.236	10	18	36	36	934.1	642.5	1021.6	73.7

was found in MnCuZnAl catalysts, showing good dispersion of the excess metal oxides.

The Mn-doping greatly influenced the reducibility of CuZnAl-based catalysts. As can be seen from Fig. 2(A), the reduction temperature of MnZnAl is much higher than CuZnAl, showing the MnO<sub>x</sub> is much less reducible than CuO, which consists with previous report [19]. However, the reduction peaks ( $T_{max}$ ) of Mn-doped CuZnAl catalysts shifted toward low temperature. The  $T_{max}$  drops dramatically from 273 °C of CuZnAl to 190 °C of MCZA50 with the increasing of Mn/Cu ratio. While further increase of Mn/Cu ratio induced increasing of the  $T_{max}$ . The MCZA50 with the optimum Cu: Mn molar ratio of about 1:1 showed the highest reducibility among the catalysts we investigated. This phenomenon may be attributed to the formation of spinel-like structure of mixed oxide as the XRD revealed. The formation of ZnMn<sub>2</sub>O<sub>4</sub> phase is also beneficial to the reduction of CuO, as the MnZnCu is observed much reducible than CuZnAl.

The Mn-doping is also beneficial to the dispersion of Cu on the surface. The surface Cu content is much lower than bulk content (27% vs 36%) in the sample CuZnAl which without Mn doping (Table 1). The deviation ( $100\% \times (Cu_{bulk} - Cu_{surface})/Cu_{bulk}$ ) is as large as 25.0%. For the Mn doped samples, the deviation sharply decreased to around 10%, even zero ( $Cu_{bulk} = Cu_{surface}$ ) in the sample of MCZA75. This phenomenon may be attributed to the formation of Cu<sub>x</sub>Zn<sub>1-x</sub>Mn<sub>2</sub>O<sub>4</sub> solid solution as XRD patterns revealed.

a Pore size; b Pore volume.

Noticing that the variation of  $T_{max}$  is quite consistent with the trend of surface Cu dispersion, we suggest that the high dispersed surface CuO is much more reducible than bulk CuO, and the reduction is mainly related to the proportion of surface copper, as Fig. 2(B) shows. Another interesting thing is, the decreasing of reduction peak by Mn doping is much greater than other metal ions doped counterparts, such as Ni and Mg (not shown here). This may be related to the inner redox equilibrium ( $Cu^{2+} + Mn^{3+} \leftrightarrow Cu^+ + Mn^{4+}$ ). The fast electron-exchange between lattice ions made the manganese ion an electronic conduction medium and further enhanced the reducibility of copper oxides. Meantime, copper also influenced the reduction of manganese. With the increasing of Cu/(Mn + Cu) ratio, the H<sub>2</sub> consumed by Mn increased, showed more reducibility of manganese (Table S1).

The N<sub>2</sub> adsorption-desorption analysis results of fresh catalysts are summarized in Table 1. It is clear that Mn doping could affect the BET

surface area to a great extent that all of the Mn-doped catalysts have a surface area two times larger than the pristine CuZnAl. More importantly, the doping of manganese largely enhanced the dispersion of copper which is the most active element among the four metals. Those are undoubtedly in favor of AWS activity for offering more active sites.

The XPS results of freshly prepared samples are also summarized in Table 1. All samples presents the principal Cu 2p<sub>3/2</sub> peak around 934.1 eV together with a broad satellites between 940 and 945 eV, which are characteristics of Cu<sup>2+</sup> species. Differ from our previous work on CuMnCo catalysts [20], the internal reduction of Cu<sup>2+</sup> by Mn<sup>3+</sup> seems not happened or severely suppressed in the fresh catalysts. It may attribute to the relatively low copper content and in presence of zinc as suggested by Fierro etc. [21]. The binding energy of Mn 2p<sub>3/2</sub> ranging from 642.1 to 642.5 eV indicates the presence of both Mn<sup>3+</sup> and Mn<sup>4+</sup> [22]. With the increasing of Mn content, the  $E_B$  value increased showed larger proportion of Mn<sup>4+</sup>. While in the used catalysts, the  $E_B$  value is below 642.0 eV (Table S2), demonstrates a mixture of Mn<sup>2+</sup> and Mn<sup>3+</sup> on the surface.

### 3.2. Catalytic performance in AWS reaction

The AWS reaction using propanal as model compound were carried out at 260 and 300 °C respectively over mixed oxide catalysts after in-situ hydrogen reduction and data was collected after 2 h reaction. As can be seen from Table 2, for the ternary mixed oxide catalysts, CuZnAl showed much more activity than MnZnAl, which indicates Cu is the more active element. According to Wen etc. [8], Cu is the most suitable candidate for this reaction, even better than noble metals. Although manganese itself has the much lower activity, it can obviously enhance the performance of Cu catalyst, therefore, CuMnZn showed the highest activity among the ternary mixed oxide catalysts.

a C: propanal conversion; S<sub>A</sub>: selectivity of propionic acid; S<sub>B</sub>: selectivity of propyl alcohol; S<sub>C</sub>: selectivity of condensation products.

b reaction atmosphere: 9 ml/min N<sub>2</sub> + 1 ml/min H<sub>2</sub>;

For the quaternary mixed oxides, the conversion of propanal increased with the increasing of Mn/(Mn + Cu) molar ratio from 0 to 50%. Further increasing of Mn content induced decreasing of AWS activity, which may ascribe to the lower content and dispersion of Cu. However, we also noticed that the trend of activity happens to match with the  $T_{max}$  in TPR which shown in Fig. 2. If it is possible that the

**Table 2**  
The catalytic performance at 260 and 300 °C respectively.

Catalysts	Cu dispersion (%)	260 °C				300 °C			
		C (%) <sup>a</sup>	S <sub>A</sub> (%)	S <sub>B</sub> (%)	S <sub>C</sub> (%)	C (%)	S <sub>A</sub> (%)	S <sub>B</sub> (%)	S <sub>C</sub> (%)
CuZnAl	8.90	15.39	88.6	11.4	0	25.4	96.21	3.79	0
MnZnAl	–	3.50	97.39	0.79	1.82	12.2	98.03	1.26	0.71
MnZnCu	35.9	28.22	87.93	12.07	0	35.5	96.26	3.74	0
MnCuAl	34.5	12.21	90.17	9.18	0.65	18.9	95.58	4.42	0
MCZA25	24.3	18.17	93.36	6.64	0	37.7	97.34	2.66	0
MCZA50	55.6	20.74	96.63	3.37	0	45.3	97.27	2.73	0
MCZA65	43.0	18.33	95.55	3.20	1.25	30.4	96.47	2.67	0.86
MCZA75	30.0	14.43	94.35	2.89	2.76	21.2	96.28	2.57	1.15
MCZA50 <sup>b</sup>	55.6	62.34	25.60	74.4	0	55.1	60.40	39.6	0

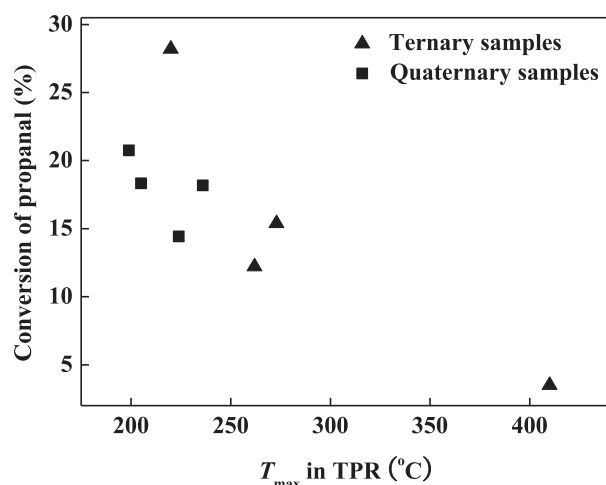


Fig. 3. The relationship between activity and reducibility.

reducibility is more essential than the Cu dispersion to the AWS activity? Therefore, we reexamined the ternary samples. As the results show, although MnZnCu and MnCuAl have the similar Cu dispersion of around 35% (Table 2), they showed completely different activity. MnCuAl and CuZnAl showed similar activity but have big difference in Cu dispersion. As it shown in Fig. 3, the AWS activity is more likely related to the reducibility of catalyst, which demonstrates a redox mechanism may be involved and the reduction of CuO is one of the steps in the catalytic cycle.

The main by-product on CuZnAl-based catalysts is propyl alcohol, which is also strongly influenced by Mn/Cu molar ratio. Compare to the pristine CuZnAl, Mn-doped samples showed higher propionic acid selectivity especially at low temperature, which may attributes to different copper species (Fig. 1S). However, the exceeding of Mn content induced the production of condensation compounds, which slightly decreases the selectivity of propionic acid. Additionally, it's also noteworthy that propyl alcohol selectivity is also greatly influenced by temperature. As shown in Table 2, the selectivity of propyl alcohol declined sharply with the temperature increase from 260 °C to 300 °C especially under H<sub>2</sub>-containing atmosphere. We speculate that hydrogenation reaction is strongly exothermic ( $\Delta_r H_m^\circ$  is estimated to  $-73.9$  kJ/mol at 300 °C), therefore higher temperature is detrimental to it but favor of the reverse reaction of dehydrogenation, and hence decreases the propyl alcohol selectivity. According to our calculation, the  $\Delta_r G_m^\circ$  at 260 °C and 300 °C are  $-8.18$  kJ/mol and  $1.89$  kJ/mol respectively. In fact, the activity of propanal hydrogenation is much higher than AWS reaction and strongly affected by temperature as the last entry in Table 2 revealed. In addition, only trace of in-situ CO/CO<sub>2</sub> detected implied almost no steam reforming reaction occurred over all of these catalysts at this reaction temperature.

#### 4. Conclusions

We showed that Mn promoted CuZnAl catalysts, prepared by coprecipitation method are active and highly selective for AWS reaction using propanal as model compound. Doping of manganese in CuZnAl strongly raised the BET surface area, Cu surface dispersion and reducibility, therefore higher activity. This promotion effect may be attributed to the formation of spinel-like phase of mixed oxides. The most favorable Mn/Cu molar ratio is around 1:1.

Both catalyst composition and reaction temperature influenced the product selectivity significantly. Appropriate Cu/(Mn + Cu) ratio results in suppressing the hydrogenation of propanal to propyl alcohol or condensation, and thereby, enhanced the selectivity of propionic acid. High temperature is favor of the endothermic propyl alcohol

dehydrogenation process rather than the exothermic process of propanal hydrogenation. Thus, higher temperature is beneficial to a higher selectivity of propionic acid. At low temperature, more than 96% of propionic acid selectivity obtained over Mn doped CuZnAl catalysts.

#### Declaration of Competing Interest

The authors declare that they have no known competing financial interests or personal relationships that could have appeared to influence the work reported in this paper.

#### Acknowledgements

The project was supported by the Fundamental Research Funds for the Central Universities (JZ2017HGTB0231), the National Natural Science Foundation of China (21406045), the Natural Science Foundation of Anhui Province (1508085QB46).

#### Authorship contribution statement.

All persons who meet authorship criteria are listed as authors, and all authors certify that they have participated sufficiently in the work, including participation in the Conceptualization, Methodology, Data curation, Writing-Original draft preparation, Writing-Reviewing, Investigation, Supervision, Visualization and Editing.

Tongqi Ye: Conceptualization, Methodology, Writing-Reviewing and Editing.

Yue Ai: Conceptualization, Data curation, Methodology, Writing-Reviewing, Writing - Original draft preparation and Editing.

Bao Chen: Investigation, Editing, Writing - Original draft preparation.

Yuewen Ye: Methodology, Editing.

Jia Sun: Visualization.

Ling Qin: Supervision.

Xin Yao: Editing.

#### Appendix A. Supplementary data

Supplementary data to this article can be found online at <https://doi.org/10.1016/j.catcom.2020.106262>.

#### References

- [1] Y. Wan, Z.K. Wu, H. Yu, S. Han, Y.G. Wei, Highly efficient oxidation of alcohols to carboxylic acids using a polyoxometalate-supported chromium(III) catalyst and CO<sub>2</sub>, *Green Chem.* 22 (2020) 3150–3154.
- [2] T.P. Brewster, W.C. Ou, J.C. Tran, K.I. Goldberg, S.K. Hanson, T.R. Cundari, D. M. Heinekey, Iridium, rhodium, and ruthenium catalysts for the “aldehyde-water shift” reaction, *ACS Catal.* 4 (2014) 3034–3038.
- [3] T.P. Brewster, J.M. Goldberg, J.C. Tran, D.M. Heinekey, K.I. Goldberg, High catalytic efficiency combined with high selectivity for the aldehyde-water shift reaction using (Para-cymene)ruthenium Precatalysts, *ACS Catal.* 6 (2016) 6302–6305.
- [4] T. Corona, A. Company, Nitrous oxide activation by a cobalt(II) complex for aldehyde oxidation under mild conditions, *Dalton Trans.* 45 (2016) 14530–14533.
- [5] T.L. Stuchinskaya, I.V. Kozhevnikov, Novel efficient catalysts based on Ru or Pd oxide for selective liquid-phase oxidation of alcohols with nitrous oxide, *Catal. Commun.* 4 (2003) 609–614.
- [6] N. Xiang, P. Xu, N. Ran, T. Ye, Production of acetic acid from ethanol over CuCr catalysts via dehydrogenation-(aldehyde-water shift) reaction, *RSC Adv.* 7 (2017) 38586–38593.
- [7] L.M. Orozco, M. Renz, A. Corma, Carbon–carbon bond formation and hydrogen production in the Ketonization of aldehydes, *ChemSusChem.* 9 (2016) 2430–2442.
- [8] W.-C. Wen, S.C. Eady, L.T. Thompson, Oxide supported metal catalysts for the aldehyde water shift reaction: elucidating roles of the admetal, support, and synergies, *Catal. Today* 355 (2020) 199–204.
- [9] B.E. Martin, A. Petric, Electrical properties of copper–manganese spinel solutions and their cation valence and cation distribution, *J. Phys. Chem. Solids* 68 (2007) 2262–2270.
- [10] D. Li, Q. Yu, S.S. Li, H.Q. Wan, L.J. Liu, L. Qi, B. Liu, F. Gao, L. Dong, Y. Chen, The remarkable enhancement of CO-pretreated CuO-Mn<sub>2</sub>O<sub>3</sub>/gamma-Al<sub>2</sub>O<sub>3</sub> supported catalyst for the reduction of NO with CO: the formation of surface synergetic oxygen vacancy, *Chem. Eur. J.* 17 (2011) 5668–5679.
- [11] G.J. Hutchings, R.G. Copperthwait, F.M. Gottschalk, R. Hunter, J. Mellor, S. W. Orchard, T. Sangiorgio, A comparative evaluation of cobalt chromium oxide,

- cobalt manganese oxide, and copper manganese oxide as catalysts for the water-gas shift reaction, *J. Catal.* 137 (1992) 408–422.
- [12] T. Fukunaga, N. Ryumon, N. Ichikuni, S. Shimazu, Characterization of CuMn-spinel catalyst for methanol steam reforming, *Catal. Commun.* 10 (2009) 1800–1803.
- [13] J. Papavasiliou, G. Avgouropoulos, T. Ioannides, Combined steam reforming of methanol over Cu–Mn spinel oxide catalysts, *J. Catal.* 251 (2007) 7–20.
- [14] M.R. Morales, B.P. Barbero, L.E. Cadús, Total oxidation of ethanol and propane over Mn–Cu mixed oxide catalysts, *Appl. Catal. B: Environ.* 67 (2006) 229–236.
- [15] Q. Liu, Z.F. Zhang, B.S. Liu, H. Xia, Rare earth oxide doping and synthesis of spinel  $ZnMn_2O_4$ /KIT-1 with double gyroidal mesopores for desulfurization nature of hot coal gas, *Appl. Catal. B: Environ.* 237 (2018) 855–865.
- [16] X.D. Zhang, Z.S. Wu, J. Zang, Z.D. Zhang, Hydrothermal synthesis and characterization of nanocrystalline Zn–Mn spinel, *J. Phys. Chem. Solids* 68 (2007) 1583–1590.
- [17] Y.L. Zhao, C.H. Zhao, Y. Tong, Spinel-structured Ni-free  $Zn_{0.9}Cu_xMn_{2.1-x}O_4$  ( $0.1 \leq x \leq 0.5$ ) thermistors of negative temperature coefficient, *J. Electroceram.* 31 (2013) 286–290.
- [18] M. M. G. Francisco, L. Federico, B. Enrique, P. Heriberto Pedro,  $Zn_{x-1}Cu_xMn_2O_4$  Spinels; synthesis, structural characterization and electrical evaluation, *J. Mexican. Chem. Society* 54 (2010) 2–6.
- [19] Y. Tanaka, T. Utaka, R. Kikuchi, T. Takeguchi, K. Sasaki, K. Eguchi, Water gas shift reaction for the reformed fuels over Cu/MnO catalysts prepared via spinel-type oxide, *J. Catal.* 215 (2003) 271–278.
- [20] T.-Q. Ye, Z.-X. Zhang, Y. Xu, S.-Z. Yan, J.-F. Zhu, Y. Liu, Q.-X. Li, Higher alcohol synthesis from bio-syngas over Na-promoted CuCoMn catalyst, *Acta Phys. -Chim. Sin.* 27 (2011) 1493–1500.
- [21] G. Fierro, S. Morpurgo, M. Jacono, M. Inversi, I. Pettiti, Preparation, characterisation and catalytic activity of CuZn-based manganites obtained from carbonate precursors, *Appl. Catal. A: Gen.* 166 (1998) 407–417.
- [22] P. Porta, G. Moretti, M. Musicanti, A. Nardella, Copper-manganese mixed oxides: formation, characterization and reactivity under different conditions, *Solid State Ionics* 63-65 (1993) 257–267.